School of Dentistry Faculty Research and Publications

Dentistry, School of

7-2020

Electrical And Mechanical Properties of BZT – xBCT Lead-Free Piezoceramics

Raziye Hayati

Mohammad Fayazi

Hadi Diargar

Mohammad Kaveh

Lobat Tayebi

Electrical And Mechanical Properties of BZT – xBCT Lead-Free Piezoceramics.

Raziye Hayati
Department of Materials Engineering, Yasouj University, Yasouj, Iran
Mohammad Fayazi
Department of Materials Engineering, Yasouj University, Yasouj, Iran
Hadi Diargar
Department of Materials Engineering, Yasouj University, Yasouj, Iran
Mohammad Kaveh
Department of Materials Engineering, Yasouj University, Yasouj, Iran
Lobat Tayebi
School of Dentistry, Marquette University, Milwaukee, WI

Abstract

In this study, lead-free $(1 - x)Ba(Zr_{0.2}Ti_{0.8})O3 - x(Ba_{0.7}Ca_{0.3})TiO_3$ compositions are synthesized via conventional solid oxide route, and the ceramics are fabricated with normal sintering in air. The effects of composition fluctuations on dielectric, piezoelectric, and mechanical properties are investigated.

The phase structure and the microstructure are analyzed with X-ray diffraction and scanning electron microscopy. The best dielectric and piezoelectric properties of ε_r = 11 207 and d_{33} = 330 pC/N were obtained for BZT−0.35BCT and BZT−0.5BCT ceramics, respectively. The mechanical behavior—in terms of Vickers hardness and compressive and flexural strengths—was investigated, and the best mechanical behavior was found in the vicinity of the phase transition boundary with x values between 0.5 and 0.6.

INTRODUCTION

Due to the ability to exchange between the electrical and mechanical energies, piezoelectric materials are widely used in a variety of applications such as sensors, actuators, and transducers.[1] Among these functional materials, lead-based compositions—specifically, $Pb(Zr_xTi_{1-x})O_3$:PZT—have attracted much attention because of their superior piezoelectric and electromechanical properties.[2] However, the cumulative toxicity of lead and the public anxiety about human health and environmental concerns persuaded researchers to look for non-Pb piezoelectric materials.[3] In 2004, a publication by Saito et al,[5] which was an answer to the severe lead-restrictive legislations of European Union, stimulated the scientific activities in the piezoelectric society.[6]

Among lead-free piezoelectric materials, $(K_xNa_{1-x})NbO_3$:KNN,[7] $(Bi,Na)TiO_3$:BNT,[8] $(Ba_{1-x}Ca_x)(Ti_{1-x}Zr_x)O_3$:BCZT,[9] and their solid solutions are potential candidates for replacing PZT and other Pb-based materials. In 2009, the pseudobinary solid solution of $Ba(Zr_{0.2}Ti_{0.8})O_3 − x (Ba_{0.7}Ca_{0.3})TiO_3$, referred to as BZT − xBCT, was introduced by Liu and Ren.[10] The BCZT composition with piezoelectric coefficients higher than PZT-based ceramics ($d_{33} \approx 620$ pC/N for x = 0.5),[10] large blocking force values,[11] and high cycling stability[12] is a good candidate for actuator applications.[13] Despite its outstanding piezoelectric properties, BCZT suffers from some limitations, including high processing temperatures[14] and low T_C, which limits the usable working temperature to less than 90°C.[15]

The actuating process involves the intermittent domain switching in the ferroelectric phase of the piezoelectric material, which results in cyclic inelastic deformation and joule heating. These phenomena influence the mechanical integrity by stimulating the crack growth. In addition, for electronic devices, the mechanical parameters—such as hardness, strength, and fracture toughness—are of considerable importance.[16] As a result, for actuator applications, investigating the mechanical properties, like crack propagation and strength, is also important considerations.[17]

Although the mechanical behavior of PZT and other lead-free piezoceramics have been studied in some publications,[17, 19, 21] there are a few publications regarding the mechanical properties of BCZT compositions; the majority of studies focused on the mechanisms of large piezoelectricity[23] and investigated the effects of dopants and solid solutions on electrical behaviors. Sirvinas et al studied the electrical and mechanical properties of BZT−0.5BCT and concluded that the values of hardness, modulus, and fracture toughness were higher than PZT ceramics.[25] In another study, Adhikari et al investigated the effect of nano-sized Al_2O_3 on ferroelectric and mechanical properties of BZT−50BCT piezoceramics. They reported a flexural strength of 92 MPa for BCZT with 1 vol.% Al_2O_3 addition.[26] Coondoo et al compared the mechanical properties of sol-gel synthesized BZT−50BCT with those of conventional oxides method. They concluded that the synthesis method controls the grain size to

influence the mechanical properties, and that the chemically synthesized BCZT with larger values of hardness and Young's Modulus showed lower piezoelectric coefficients.[27]

In the above-mentioned studies, the attention has been focused on the mechanical properties of BZT–50BCT composition. However, the phase diagram of BZT – xBCT covers a variety of compositions with different crystal structures and interesting properties. Hence, in this work, the electrical and mechanical properties of BZT – xBCT composition with x values in the range 0.35-0.6—corresponding to different crystal structures—are studied.

EXPERIMENTAL PROCEDURE

Ba(Zr$_{0.2}$Ti$_{0.8}$)O$_3$ – x (Ba$_{0.7}$Ca$_{0.3}$)O$_3$ compositions with x = 0.35, 0.45, 0.5, and 0.6 (referring to BCZT35, BCZT45, BCZT50, and BCZT60, respectively) were synthesized via solid-state sintering route. The raw materials of BaCO$_3$, CaCO$_3$, TiO$_2$, and ZrO$_2$ (99.5%, Merck company) were mixed based on the stoichiometric formula and ground for 5 hours in a high energy mill at 180 rpm in ethanol using zirconia cups and balls. The dried powders were calcined at 1300°C for 4 hours (heating rate 3°C/minute), and another milling process of 2 hours was performed at 250 rpm. The powders were shaped into disks of 10 mm in diameter and 1.5-2 mm in thickness, and a subsequent pressure of 250 MPa was applied with cold isostatic pressing (CIP, K303, Iran). The sintering was performed in zirconia crucibles at 1500°C (heating rate of 5°C/minute) for 2 hours.

The phase composition of sintered and subsequently crushed powders was characterized using Cu$k\alpha$ radiation (XRD; D8 Advance, Bruker Inc), and the microstructures of thermally etched samples were analyzed with Scanning Electron Microscopy (SEM, TESCAN-Vega 3, Czech Republic). The average grain size of at least 200 grains was calculated by the mean intercept length method using LINCE software.

The Archimedes' method was used to measure the bulk density of polished samples. To measure the dielectric and piezoelectric properties, the samples were electroded with silver paste, and the poling process was performed at room temperature by applying an electric field of 3 kV/mm for 30 minutes. The dielectric properties were measured with a precision LCR meter at a frequency of 1 KHz, and the small signal d_{33} was measured with a SINOCERA d_{33} meter (Model YE2730) at a frequency of 1 Hz.

The compressive strength test was performed on cylindrical samples with a diameter of 7-8 mm and a thickness of 10 mm using a DMG Universal testing machine (Model 7166, United Kingdom) with a speed of 0.5 mm/minute (based on ASTM C1428[28]). Young's Modulus and toughness were calculated from the slope and area of stress-strain curves, respectively. Disk-shaped samples with a diameter of 7-8 mm and a thickness of 1-2 mm were selected for the Vickers hardness test (MHV1000Z), and the test was performed with a load of 200 g and a dwell time of 20 seconds (based on ASTM C1327[28]). The flexural strength of the samples was measured based on three-point method with a Zwick/Roell Universal testing machine (based on ASTM C1161[28]). Dimensions of the specimens before sintering were 30 mm × 5 mm × 5 mm (length × width × thickness).

RESULTS & DISCUSSION

Figure 1 demonstrates the SEM images of BCZT powders that were synthesized at 1300°C, followed by high energy milling with 250 rpm for 2 hours. As seen, the particle size is less than 200 nm and a

uniform powder width is used for sintering. As the powder characteristics are crucial parameters in compaction and sintering, these factors are considered in this work.
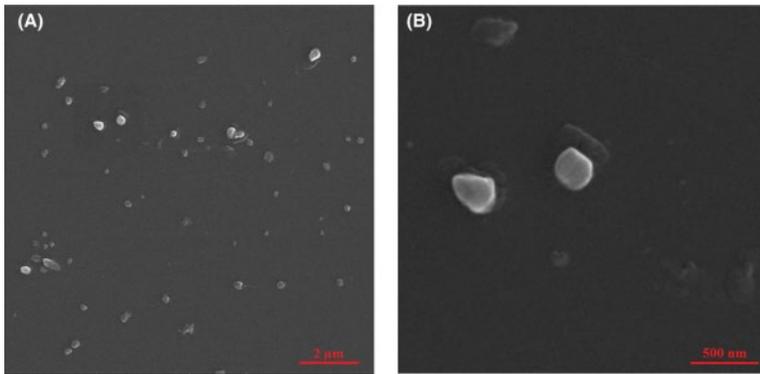
Figure 1 Scanning electron microscopy micrographs of the synthesized BCZT powder after high energy milling at 250 rpm for 2 h, with two different magnifications 14.5 kx (A) and 65.0 kx (B)

The XRD patterns of BZT − xBCT samples are shown in Figure 2. According to the patterns, all the samples possess pure perovskite structure with no signs of secondary phases. The inset of Figure 2A shows the shift of $2\vartheta = 31°$ peaks to higher angles with increasing the x value, which indicates the lattice contraction due to increasing the Ca and decreasing the Zr content of the compositions.
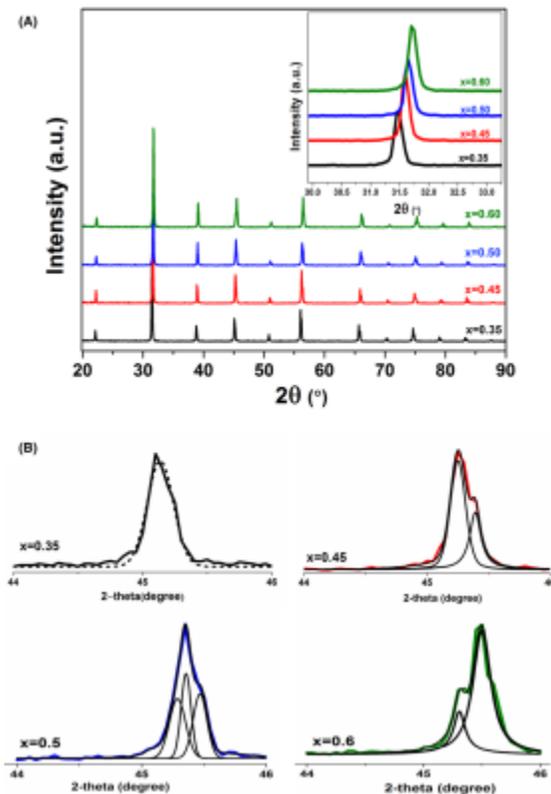
Figure 2 A, The XRD pattern of BZT − xBCT samples sintered at 1500°C; the inset shows the shift of (110) peaks with increasing x (B) Magnification of the peaks at $2\theta = 45$ and the corresponding results of fitting with software. Correction added on 20th May, after first online publication: Figure 2a was replaced to correct scale of the XRD patterns

Mane et al believes that the reduction in Zr^{4+} with increasing the BCT content is the reason for this kind of peak shifts in the XRD patterns of BZT − xBCT compositions, as compared with the less chemically stable Ti^{4+}.[29] Considering the recent phase diagram of BZT − xBCT[30] and fitting the peaks of $2\vartheta = 45°$ by using Origin Pro 2015 software with a Gaussian function, the different phase structures of BZT − xBCT compositions are distinguished and demonstrated in Figure 2B. Accordingly, BCZT35—which is said to lie in the rhombohedral side of the phase diagram—is identified with a single (200) peak, while for x = 0.45—which is in the vicinity of the transition region between rhombohedral and orthorhombic phases—the structure is a bit different. The splitting of the peaks in BCZT60 well agrees with tetragonal structure, and the coexistence of tetragonal and orthorhombic phases is an indication of BCZT50, which is said to be precisely located at the MPB region.

The plots of variations in density with composition are presented in Figure 3. The samples are dense, with relative density values higher than 97%, which are in good agreement with the results of other studies. As the BCT content of the solid solution increases, the bulk density decreases, but due to lower theoretical values, the relative density shows an ascending trend with increasing the x value. The SEM micrographs of BZT − xBCT samples are demonstrated in Figure 4. The images are from the polished and thermally etched surfaces. According to these figures, the microstructures are dense and uniform. The average grain size increases from ≈7 μm for x = 0.35 to about 14-18 μm for the other samples, which is in good agreement with previous results of Bijalwan et al for conventionally sintered BZT−0.5BCT.[31] On one hand, according to Tian et al, as the Ca content of the $(Ba_{1-x}Ca_x)(Zr_{0.1}Ti_{0.9})O_3$ composition increases, the coupling between Ca^{2+} and Ti^{4+} ions impede the grain boundary movement and results in smaller grains.[32] On the other hand, Li et al declares that in this composition, the higher Ca content results in larger grains.[33] In addition, Wu et al showed that in $(Ba_{0.85}Ca_{0.15})(Zr_xTi_{1-x})O_3$ compositions, with increasing the Zr contents, the grains become larger and more cubic phase is prone to exist.[34] In the BZT − xBCT compositions, increasing the x value leads to an increase in Ca content and decrease in the Zr content, but the final microstructure is a result of a balance between the Ca and Zr contents of the compositions. The increase in grain size with increasing the amount of BCT up to 50% is somewhat consistent with previous report of Li et al.[35] However, they reported that in BZT − xBCT compositions with x values higher than 0.5, the grain size decreases, which is in contrast with our results.
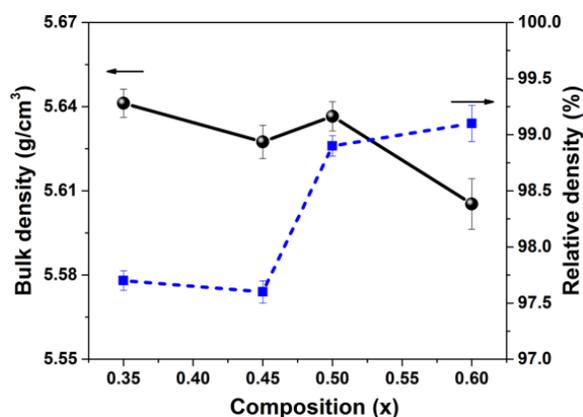
Figure 3 The variations in density with composition for BZT − xBCT samples sintered at 1500°C for 2 h
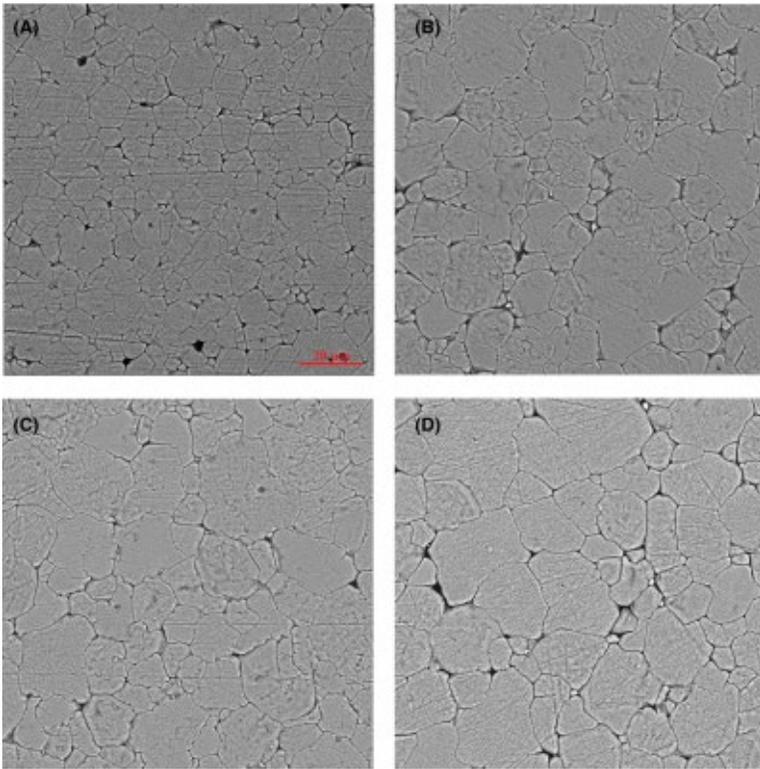
Figure 4 Scanning electron microscopy micrographs of polished and thermally etched surfaces of BZT − xBCT ceramics sintered at 1500°C, (A) x = 0.35, (B) x = 0.45, (C) x = 0.5, and (D) x = 0.6

The macroscopic driving force of solid-state sintering is the reduction in the excess energy associated with surfaces. This is accompanied by the elimination of solid-vapor interfaces (densification) and the increase in the average grain size (coarsening)[36]; therefore, smaller particles impose a larger driving force, leading to better densification without considerable grain coarsening. In this study, the dense microstructure of the BCZT samples, which consists smaller grains than majority of the previous works,[24, 37] can be related to the smaller particle size of the initial powder before sintering, as well as the proper control of the sintering parameters—ie, material and process variables—to achieve the optimum electrical and mechanical properties.

The dielectric plots of ε_r-T and tanδ-T are shown in Figure 5. As seen, except for BCZT35, in which T_C is in the vicinity of room temperature, the broad peaks of tetragonal-cubic transitions are clearly distinguished in the other three samples. In addition, the shift of T_C to lower temperatures is accompanied by an increase in the room temperature permittivity, as ε_r drastically increased from 3000 for x = 0.6 to 11 000 for x = 0.35. It should be noted that the Curie temperature of the BZT − xBCT samples of this study is lower than the results of previous reports.[35, 38] This can be attributed to the smaller particle size of the initial powder and the resultant finer microstructure of the samples, as demonstrated in the SEM images of Figure 4.
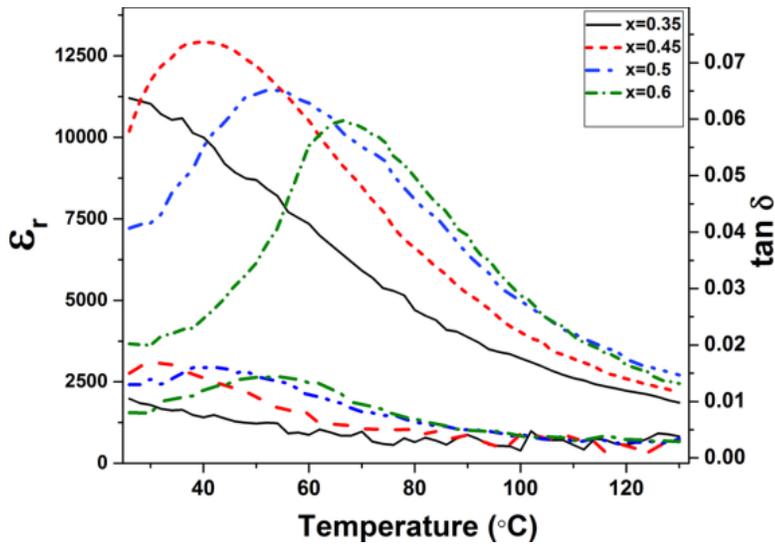
Figure 5 Temperature-dependent dielectric properties of BZT − xBCT compositions measured at the frequency of 1 KHz

The variations in dielectric constant and small signal d_{33} with composition are demonstrated in the plots of Figure 6. Accordingly, the higher Zr contents are accompanied with lower ε_r values, but the piezoelectric coefficient shows a different trend with the maximum value of 330 pC/N for BZT−0.5 BCT composition, located in the MPB region. Grain size and density are the two important parameters affecting the dielectric and piezoelectric properties, as declared in the literature. According to HaO et al, the variations in grain size (d) influence the domain size (t) with the formula expressed as $d = \left[\left(\frac{\sigma}{\varepsilon^* P_s^2}\right) t\right]^{1/2}$, in which σ, ε^*, and P_s denote the energy density of the domain wall, spontaneous polarization, and dielectric constant, respectively.[40] Larger grains facilitate the domain wall switching and result in higher piezoelectric coefficients. Therefore, in this study, the higher piezoelectric constant of the compositions with x = 0.45 to x = 0.6, compared with x = 0.35, can be related to the simultaneous effect of dielectric constant and grain size. However, for x values between 0.45 and 0.6, the negligible difference in grain size has paled the effect of grain size on piezoelectric properties. Besides, the various amounts of Zr and Ca in BZT − xBCT compositions result in different crystal structures, as indicated in the XRD section, and the microstructure was also affected accordingly. As a result, the different piezoelectric behavior of these four compositions can also be related to these structural differences at room temperature. Therefore, the BZT−0.5BCT composition with coexistence of ferroelectric phases has the largest d_{33} value of 330 pC/N.
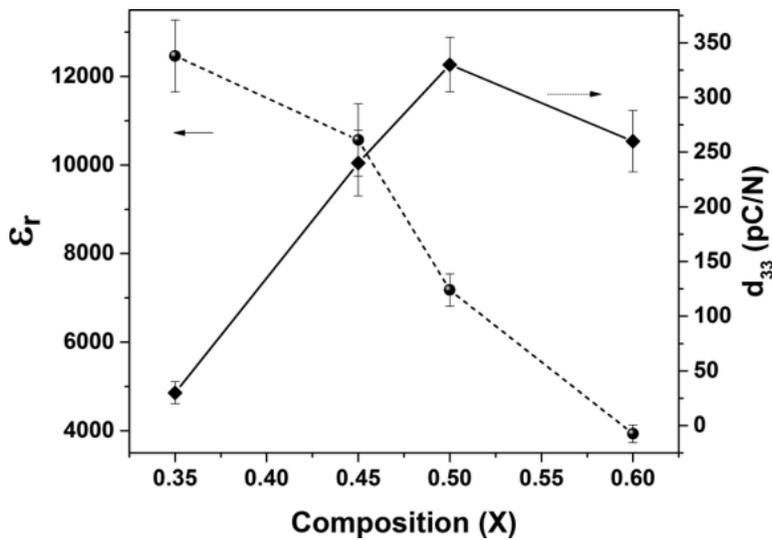
Figure 6 The plots of variations in room temperature εr and d33 with composition

Mechanical properties, in terms of Vickers hardness and compressive and flexural strengths, were investigated. The plots of variations in microhardness and bending strength with composition are shown in Figure 7.
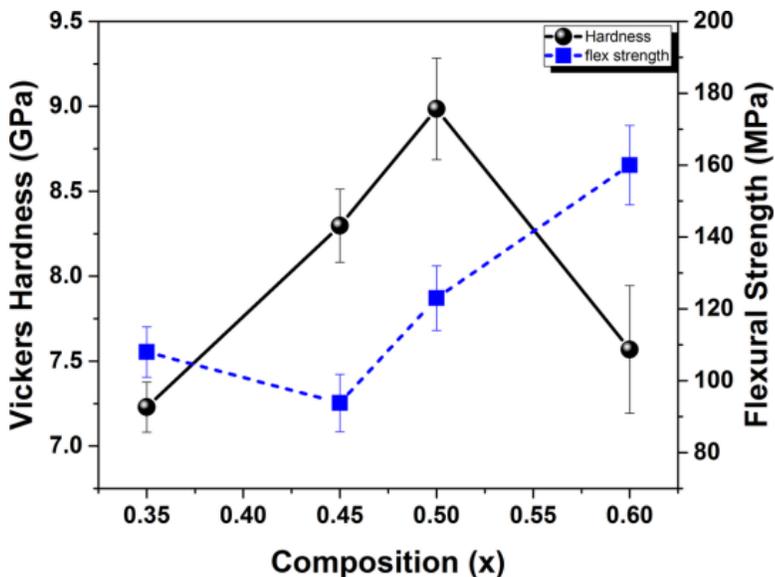
Figure 7 The variations in hardness and flexural strength with composition; the inset shows the plot of flexural modulus versus composition

As seen, with increasing the x value in BZT − xBCT composition, the hardness increased up to $x = 0.5$, after which, the value demonstrates a descending trend. Although the Hall-Petch equation[41] predicts higher hardness values for fine-grained microstructures, the BZT−0.35BCT composition with smallest grains has the lowest hardness value. The flexural strength shows a different trend, with the highest value of about 160 MPa for BZT−60BCT sample and a minimum at $x = 0.45$. The bending strength of the ceramics is highly dependent on pore size and density.[20] In this study, due to the similar trends of variations in flexural strength and density with composition, the considerable value of bending strength in BCZT60 sample is justified with its higher density. It should be noted that the flexural

strength and hardness of this sample is similar to the natural bone and is higher than the values reported for many bioceramics.[42-45]

Adhikari et al investigated the mechanical properties of BZT−50BCT ceramics with Al_2O_3 additive. The amounts of hardness (741.5 MPa) and flexural strength (92 MPa) that they reported for BCZT ceramics with 1 Vol% Al_2O_3 were lower than the corresponding values of this work.[26] However, Sirvinas et al reported a hardness of 11.6 GPa for BZT−0.5 BCT samples sintered at 1500°C for 5 hours.[25] The stress-strain curves and the corresponding plots of compressive strength, toughness, and compressive modulus of BZT − xBCT samples are shown in Figure 8. According to Figure 8A, the linear elastic part of the curves is accompanied by a nonlinear ferroelastic region, which is more pronounced for BCZT45. Tan at al. attributed the beginning of the stress-strain curves of piezoceramics to the ferroelectric domain switching after applying the compressive forces.[21] Besides, this nonlinear region and the corresponding microscopic domain switching would lead to higher macroscopic nonreversible remanent deformation.[21, 46] Therefore, BCZT45 is expected to show the largest piezoelectric strain values, which is in good agreement with the results of Ehmke et al, in which they reported the highest piezoelectric strain for BZT−0.45BCT composition.[47] As demonstrated in the inset of Figure 8A, the BCZT50 has a much higher compressive strength compared with other compositions, which is accompanied by higher modulus and toughness for this composition.
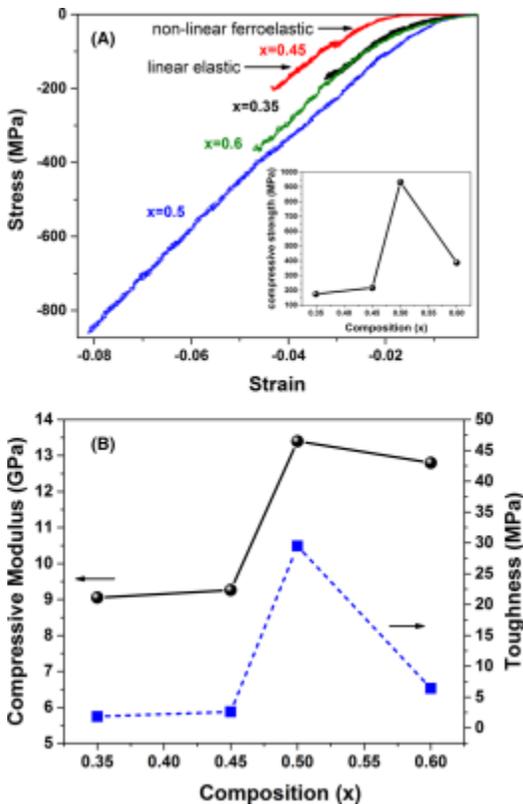
Figure 8 A, The stress-strain curves of BZT − xBCT compositions (the inset showing the variations in the compressive strength with composition). B, The plots of compressive modulus and toughness as a function of composition

Chen et al declared that density and grain size are the two competing factors affecting the compressive strength of ceramics and are related to the strength with the following equations:

1. $\sigma = \sigma_0 \exp(-k\alpha)$

2. $\sigma = \sigma_0 + kd^{-m}$.

Here, σ and σ_0 are the strengths of material with and without defects, respectively. In addition, α is the residual porosity, which is inversely proportional to the relative density, whereas d is the grain size and k and m are the experimental coefficients.[46] Accordingly, dense ceramics with less defects and smaller grains are supposed to lead to higher compressive strengths. In this work, although BCZT35 and BCZT60 have the smallest grains and the highest density, respectively, the best compressive strength of 932 MPa was obtained for BCZT50 with a low dielectric loss, high density, and moderate grain size. In addition, the compressive strengths of this study are much higher than PZT and other lead-free piezoceramics, as well as natural bone.[45, 48]

As there are only few reports on mechanical properties of BZT − xBCT compositions that considered the BZT−50BCT, it is hard to compare the results of this study with previous publications on BCZT. However, the results can be compared with lead-based and other lead-free piezoceramics. According to the literature, undoped BaTiO$_3$ ceramics that were sintered with pressure-less techniques possess Vickers hardness,[49] compressive strength, and flexural strength[50] values lower than BCZT. The substitution of Ca and Zr in the crystal structure of BT and altering the atomic bonds between the cations and oxygen ions results in different mechanical behavior in BCZT composition. Tan et al studied the electrical and mechanical properties of KNN-based ceramics and reported the mechanical properties as hardness = 2.2-5 GPa, flexural strength = 37-125 MPa, and compressive strength = 36-125 MPa.[21] In another study, Takahashi et al reported the bending strength of 185 MPa for pure BNT, which improved to 215 MPa for Nb-doped BNT piezoceramics. In addition, the results of our study are higher than the values that were reported for pure PZT with flexural strength and modulus of 85 and 1.5 MPa, respectively.[51]

CONCLUSION

Lead-free $(1 − x)$Ba(Zr$_{0.2}$Ti$_{0.8}$)O$_3$ − x(Ba$_{0.7}$Ca$_{0.3}$)TiO$_3$ ceramics were fabricated via conventional solid-state method and sintering was performed at 1500°C in air. The effects of Zr and Ca contents on electrical and mechanical properties were investigated. Accordingly, with increasing the x value, the grain size increases and Curie temperature shifts to lower temperatures as the T_C of BZT−0.35BCT composition with the highest ε_r of 11 207 moves to near room temperature. The highest d_{33} value of 330 pC/N is obtained for BZT−0.5BCT located near the phase transition region. In addition, the best mechanical behavior, in terms of microhardness and compressive and flexural strengths, was achieved for BZT − xBCT compositions with x = 0.5-0.6, which can be regarded as a promising candidate for actuator applications, as well as bone tissue engineering.

ACKNOWLEDGMENTS

REFERENCES

1. *Vats G, Vaish R. Selection of lead-free piezoelectric ceramics. Int J Appl Ceram Technol. 2014 ; 11 (5): 883 – 93.*
2. *Koruza J, Bell AJ, Frömling T, Webber KG, Wang K, Rödel J. Requirements for the transfer of lead-free piezoceramics into application. J Materiomics. 2018 ; 4 (1): 13 – 26.*
3. *Rödel J, Jo W, Seifert KTP, Anton E-M, Granzow T, Damjanovic D. Perspective on the development of lead-free piezoceramics. J Am Ceram Soc. 2009 ; 92 (6): 1153 – 77.*
4. *Long P, Yi Z. Fabrication and properties of (Ba 0.85 Ca 0.15)(Ti 0.9 Zr 0.1)O 3 ceramics and their multilayer piezoelectric actuators. Int J Appl Ceram Technol. 2017 ; 14 (1): 16 – 21.*
5. *Saito Y, Takao H, Tani T, Nonoyama T, Takatori K, Homma T, et al. Lead-free piezoceramics. Nature. 2004 ; 432 (7013): 84 – 7.*
6. *Rödel J, Webber KG, Dittmer R, Jo W, Kimura M, Damjanovic D. Transferring lead-free piezoelectric ceramics into application. J Eur Ceram Soc. 2015 ; 35 (6): 1659 – 81.*
7. *Thong H-C, Zhao C, Zhou Z, Wu C-F, Liu Y-X, Du Z-Z, et al. Technology transfer of lead-free (K, Na)NbO 3 -based piezoelectric ceramics. Materials Today. 2019 ; 29 : 37 – 48.*
8. *Reichmann K, Feteira A, Li M. Bismuth Sodium Titanate based materials for piezoelectric actuators. Materials. 2015 ; 8 : 8467 – 95.*
9. *Zhang Y, Sun H, Chen W. A brief review of Ba(Ti 0.8 Zr 0.2)O 3 –(Ba 0.7 Ca 0.3)TiO 3 based lead-free piezoelectric ceramics: past, present and future perspectives. J Phys Chem Solids. 2018 ; 114 : 207 – 19.*
10. *Liu W, Ren X. Large piezoelectric effect in Pb-free ceramics. Phys Rev Lett. 2009 ; 103 : 257602.*
11. *Brandt D, Acosta M, Koruza J, Webber K. Mechanical constitutive behavior and exceptional blocking force of lead-free BZT– x BCT piezoceramics. J Appl Phys. 2014 ; 115 : 204107.*
12. *Zhang Y, Glaum J, Ehmke MC, Blendell JE, Bowman KJ, Hoffman MJ. High bipolar fatigue resistance of BCTZ lead-free piezoelectric ceramics. J Am Ceram Soc. 2016 ; 99 (1): 174 – 82.*
13. *Hayati R, Bahrevar MA, Ebadzadeh T, Rojas V, Novak N, Koruza J. Effects of Bi 2 O 3 additive on sintering process and dielectric, ferroelectric, and piezoelectric properties of (Ba 0.85 Ca 0.15)(Zr 0.1 Ti 0.9)O 3 lead-free piezoceramics. J Eur Ceram Soc. 2016 ; 36 (14): 3391 – 400.*
14. *Hayati R, Bahrevar MA, Ganjkhanlou Y, Rojas V, Koruza J. Electromechanical properties of Ce-doped (Ba 0.85 Ca 0.15)(Zr 0.1 Ti 0.9)O 3 lead-free piezoceramics. J Adv Ceram. 2019 ; 8 (2): 186 – 95.*
15. *Acosta M, Khakpash N, Someya T, Novak N, Jo W, Nagata H, et al. Origin of the large piezoelectric activity in (1– x)Ba(Zr 0.2 Ti 0.8)O 3 – x (Ba 0.7 Ca 0.3)TiO 3 Ceramics. Phys Rev B. 2015 ; 91 : 104108.*
16. *Promsawat M, Watcharapasorn A, Jiansirisomboon S. Effects of ZnO nanoparticulate addition on the properties of PMNT ceramics. Nanoscale Res Lett. 2012 ; 7 (1): 65.*
17. *Bermejo R, Deluca M. Mechanical characterization of PZT ceramics for multilayer piezoelectric actuators. J Ceram Sci Technol. 2012 ; 3 : 159 – 68.*
18. *Nam HD, Lee HY. Electrical and mechanical properties of PZT ceramics. Ferroelectrics. 1996 ; 186 (1): 309 – 12.*
19. *James N, van den Ende D, Lafont U, Zwaag S, Groen P. Piezoelectric and mechanical properties of structured PZT-epoxy composites. J Mater Res. 2013 ; 28 (4): 635 – 41.*

20. *Takahashi H, Nagata H, Takenaka T. Mechanical bending strength of (Bi 0.5 Na 0.5) TiO 3 -based lead-Free piezoelectric ceramics. J Asian Ceram Soc. 2017 ; 5 (3): 242 – 6.*

21. *Tan Z, Xie S, Jiang L, Xing J, Chen YU, Zhu J, et al. Oxygen octahedron tilting, electrical properties and mechanical behaviors in alkali niobate-based lead-free piezoelectric ceramics. J Materiomics. 2019 ; 5 (3): 372 – 84.*

22. *Efe C, Yilmaz H, Tur YK, Duran C. Mechanical property characterization of Na 1/2 Bi 1/2 TiO 3 –BaTiO 3 ceramics. Int J Eng Res Appl. 2014 ; 5 (5): 429 – 32.*

23. *Gao J, Hu X, Zhang LE, Li F, Zhang L, Wang YU, et al. Major contributor to the large piezoelectric response in (1– x)Ba(Zr 0.2 Ti 0.8)O 3 – x (Ba 0.7 Ca 0.3)TiO 3 ceramics: domain wall motion. Appl Phys Lett. 2014 ; 104 (25): 252909.*

24. *Acosta M, Novak N Jr, Rossetti GA, Rödel J. Mechanisms of electromechanical response in (1– x)Ba(Zr 0.2 Ti 0.8)O 3 – x (Ba 0.7 Ca 0.3)TiO 3 ceramics. Appl Phys Lett. 2015 ; 107 (14): 142906.*

25. *Srinivas A, Krishnaiah RV, Niranjani VL, Kamat SV, Karthik T, Asthana S. Ferroelectric, piezoelectric and mechanical properties in lead free (0.5)Ba(Zr 0.2 Ti 0.8)O 3 –(0.5)(Ba 0.7 Ca 0.3)TiO 3 electroceramics. Ceram Int. 2015 ; 41 (2, Part A): 1980 – 5.*

26. *Adhikari P, Mazumder R, Sahoo GK. Electrical and mechanical properties of 0.5Ba(Zr 0.2 Ti 0.8)O 3 –0.5(Ba 0.7 Ca 0.3)TiO 3 (BZT–BCT) lead free ferroelectric ceramics reinforced with nano-sized Al 2 O 3. Ferroelectrics. 2016 ; 490 (1): 60 – 9.*

27. *Coondoo I, Panwar N, Alikin D, Bdikin I, Islam SS, Turygin A, et al. A comparative study of structural and electrical properties in lead-free BCZT ceramics: influence of the synthesis method. Acta Mater. 2018 ; 155 : 331 – 42.*

28. *ASTM Subcommittee C28.01 Mechanical Properties & Reliability. Processing, properties, and design of advanced ceramics and composites II. p. 45 – 58.*

29. *Mane SM, Tirmali PM, Kulkarni SB. Hybrid microwave sintering and shifting of T c in lead-free ferroelectric composition x (Ba 0.7 Ca 0.3 TiO 3)–(1– x)(BaZr 0.2 Ti 0.8 O 3). Mater Chem Phys. 2018 ; 213 : 482 – 91.*

30. *Shin D-J, Kim J, Koh J-H. Piezoelectric properties of (1– x)BZT– x BCT system for energy harvesting applications. J Eur Ceram Soc. 2018 ; 38 (13): 4395 – 403.*

31. *Bijalwan V, Tofel P, Erhart J, Maca K. The complex evaluation of functional properties of nearly dense BCZT ceramics and their dependence on the grain size. Ceram Soc. 2019 ; 45 (1): 317 – 26.*

32. *Tian Y, Chao X, Wei L, Liang P, Yang Z. Phase transition behavior and electrical properties of lead-free (Ba 1 – x Ca x)(Zr 0.1 Ti 0.9)O 3 piezoelectric ceramics. J Appl Phys. 2013 ; 113 (18): 184107.*

33. *Li W, Xu Z, Chu R, Fu P, Zang G. Polymorphic phase transition and piezoelectric properties of (Ba 1 – x Ca x) (Ti 0.9 Zr 0.1)O 3 lead-free ceramics. Physica B Condens Matter. 2010 ; 405 (21): 4513 – 6.*

34. *Wu J, Xiao D, Wu W, Chen Q, Zhu J, Yang Z, et al. Composition and poling condition-induced electrical behavior of (Ba 0.85 Ca 0.15)(Ti 1 – x Zr x)O 3 lead-free piezoelectric ceramics. J Eur Ceram Soc. 2012 ; 32 (4): 891 – 8.*

35. *Li SB, Wang CB, Ji X, Shen Q, Zhang LM. Effect of composition fluctuation on structural and electrical properties of BZT– x BCT ceramics prepared by Plasma Activated Sintering. J Eur Ceram Soc. 2017 ; 37 (5): 2067 – 72.*

36. *Rahaman MN. Ceramic processing and sintering. 2nd ed. Boca Raton, FL : CRC Press ; 2003 : 870.*

37. *Rojas V, Koruza J, Patterson EA, Acosta M, Jiang X, Liu N, et al. Influence of composition on the unipolar electric fatigue of Ba(Zr 0.2 Ti 0.8)O 3 –(Ba 0.7 Ca 0.3)TiO 3 lead-free piezoceramics. J Am Ceram Soc. 2017 ; 100 (10): 4699 – 709.*

38. *Zhang Y, Glaum J, Groh C, Ehmke MC, Blendell JE, Bowman KJ, et al. Correlation between piezoelectric properties and phase coexistence in (Ba, Ca)(Ti, Zr)O 3 Ceramics. J Am Ceram Soc. 2014 ; 97 (9): 2885 – 91.*

39. *Acosta M, Novak N, Jo W, Rödel J. Relationship between electromechanical properties and phase diagram in the Ba(Zr 0.2 Ti 0.8)O 3 – x (Ba 0.7 Ca 0.3)TiO 3 lead-free piezoceramic. Acta Mater. 2014 ; 80 : 48 – 55.*

40. *Hao J, Bai W, Li W, Zhai J. Correlation between the microstructure and electrical properties in high-performance (Ba 0.85 Ca 0.15)(Zr 0.1 Ti 0.9)O 3 lead-free piezoelectric ceramics. J Am Ceram Soc. 2012 ; 95 (6): 1998 – 2006.*

41. *Pande CS, Cooper KP. Nanomechanics of Hall-Petch relationship in nanocrystalline materials. Prog Mater Sci. 2009 ; 54 (6): 689 – 706.*

42. *Dubey AK, EA A, Balani K, Basu B. Multifunctional properties of multistage spark plasma sintered HA–BaTiO 3 -based piezobiocomposites for bone replacement applications. J Am Ceram Soc. 2013 ; 96 (12): 3753 – 9.*

43. *Sedlin ED. A Rheologic Model for cortical bone: a study of the physical properties of human femoral samples. Acta Orthop Scand. 1965 ; 36 (sup83): 1 – 77.*

44. *Soares PBF, Nunes SA, Franco SD, Pires RR, Zanetta-Barbosa D, Soares CJ. Measurement of elastic modulus and vickers hardness of surround bone implant using dynamic microindentation—parameters definition. Braz Dent J. 2014 ; 25 : 385 – 90.*

45. *Pramanik S, Agarwal A, Rai K. Development of high strength hydroxyapatite for hard tissue replacement. Trends Biomater Artif Organs. 2005 ; 19 : 46 – 51.*

46. *Chen Y, Xie S, Wang Q, Fu L, Nie R, Zhu J. Correlation between microstructural evolutions and electrical/mechanical behaviors in Nb/Ce co-doped Pb(Zr 0.52 Ti 0.48)O 3 ceramics at different sintering temperatures. Mater Res Bull. 2017 ; 94 : 174 – 82.*

47. *Ehmke MC, Ehrlich SN, Blendell JE, Bowman KJ. Phase coexistence and ferroelastic texture in high strain (1– x)Ba(Zr 0.2 Ti 0.8)O 3 – x (Ba 0.7 Ca 0.3)TiO 3 piezoceramics. J Appl Phys. 2012 ; 111 (12): 124110.*

48. *Carter DR, Hayes WC. Bone compressive strength: the influence of density and strain rate. Science. 1976 ; 194 (4270): 1174.*

49. *Panteny S, Bowen C, Stevens R. Characterisation of Barium Titanate-Silver composites, Part I: microstructure and mechanical properties. J Mater Sci. 2006 ; 41 : 3837 – 43.*

50. *Tang Y, Wu C, Wu Z, Hu L, Zhang W, Zhao K. Fabrication and in vitro biological properties of piezoelectric bioceramics for bone regeneration. Sci Rep. 2017 ; 7 : 43360.*

51. *James NK, van den Ende D, Lafont U, van der Zwaag S, Groen WA. Piezoelectric and mechanical properties of structured PZT–epoxy composites. J Mater Sci. 2013 ; 28 (4): 635 – 41.*